

CHEMISTRY

AN **ASIAN** JOURNAL

www.chemasianj.org

Accepted Article

Title: ZIF-8-Nanocrystalline Zirconosilicate Integrated Porous Material for the Activation and Utilization of CO₂ in the Insertion Reactions

Authors: Diksha Srivastava, Poonam Rani, and Rajendra Srivastava

This manuscript has been accepted after peer review and appears as an Accepted Article online prior to editing, proofing, and formal publication of the final Version of Record (VoR). This work is currently citable by using the Digital Object Identifier (DOI) given below. The VoR will be published online in Early View as soon as possible and may be different to this Accepted Article as a result of editing. Readers should obtain the VoR from the journal website shown below when it is published to ensure accuracy of information. The authors are responsible for the content of this Accepted Article.

To be cited as: *Chem. Asian J.* 10.1002/asia.202000001

Link to VoR: <http://dx.doi.org/10.1002/asia.202000001>

A Journal of



A sister journal of *Angewandte Chemie*
and *Chemistry – A European Journal*

WILEY-VCH

ZIF-8-Nanocrystalline Zirconosilicate Integrated Porous Material for the Activation and Utilization of CO₂ in the Insertion Reactions

Diksha Srivastava,^{a,b} Poonam Rani,^{a,b} and Rajendra Srivastava^{*b}

Dedication ((optional))

- [a] Diksha Srivastava, Poonam Rani
Both authors have an equal contribution
- [b] Diksha Srivastava, Poonam Rani, and Rajendra Srivastava
Department of Chemistry
Indian Institute of Technology Ropar
Rupnagar-140001, India
E-mail: rajendra@iitrpr.ac.in

Supporting information for this article is given via a link at the end of the document.

Abstract: The conversion of CO₂ to useful chemicals, especially to atom economical products, is the best approach to utilize an excess of CO₂ present in the atmosphere. In this study, a metal-organic framework ZIF-8 is integrated with nanocrystalline zirconosilicate zeolite to develop an integrated porous catalyst for the CO₂ insertion reactions. The catalyst exhibits excellent activity for the CO₂ insertion reaction of epoxide to produce cyclic carbonate in neat condition without the addition of any co-catalyst. The catalyst is stable and recyclable during the cyclic carbonate synthesis. Further, the catalyst also exhibits very good activity in another CO₂ insertion reaction to produce quinazoline-2,4(1H, 3H)-dione.

Introduction

Gaseous CO₂ present in the troposphere region of the earth is creating harmful effects on all living organisms including human beings. The anthropogenic CO₂ emission (due to the rapid industrial evolution, high demand for energy, and fossil fuels-based transportation) is mainly responsible for the increase in CO₂ level to more than 400 ppm in the atmosphere. Due to this increase in the CO₂ level, the average temperature on earth has risen by more than 1° C (since the pre-industrial era) and is expected to increase to 1.9 °C by 2050.^[1] Thus it is very important to control the CO₂ emission rate. Government agencies are making efforts to reduce the CO₂ concentration but these efforts might give limited results due to the large population and their energy demand. Thus the role of scientists has become essential to restrain the level of CO₂. There are only two possibilities by which this problem can be sorted out, (1) CO₂ capture and storage and (2) CO₂ conversion to useful chemicals and fuels. CO₂ capture and storage are possible only when the emission source emits a large concentration of CO₂.^[2, 3] Only limited success has been achieved with porous materials and liquid amine-based scrubbers for CO₂ adsorption and separation.^[4-7] The kinetic diameter of CO₂ (0.33 nm) is very similar to O₂ (0.35 nm) and N₂ (0.36 nm) which makes it very difficult to design porous materials with high CO₂ capture capacity.^[8] Therefore, the development of alternative routes for the conversion of CO₂ to useful chemicals and fuels has become extremely useful.

Only a few industrial processes based on CO₂ are known, such as; the production of urea, organic carbonates, methanol, salicylic acid, etc.^[9-16] This is due to the thermodynamic inertness of CO₂. CO₂ can be used as the source of O (a mild oxidant), CO (in urea synthesis), and C (for the synthesis of methanol, CH₄ and other fuels).^[9-15] But the most atom economy

process is the insertion of CO₂ into epoxides/amines to produce a wide range of organic compounds such as cyclic carbonate/carbamate and quinazoline-2,4(1H, 3H)-dione. In order to develop sustainable catalysts for CO₂ insertion reactions, CO₂ should be adsorbed and suitably activated. When adsorption is considered, zeolites and metal-organic frameworks (MOFs) are the most preferred materials due to their tunable porosity.^[6, 7, 16-18] Zeolites have microporosity, which makes them suitable materials for CO₂ adsorption. However, zeolites alone can not be used for CO₂ insertion reactions, due to their inability to activate CO₂. MOFs have microporosity and high surface area, therefore they are good candidates for CO₂ capture and storage. Only, a few MOFs are known in the literature, which has the ability to activate CO₂.^[19] CO₂ is an acidic molecule, and it can only be activated if the basic sites are present in the MOFs.^[20] Thus; functional MOFs having amines groups have been explored in the CO₂ insertion reactions.^[21-23] Further, zeolites based materials have been also explored in cyclic carbonate synthesis by functionalizing zeolites with amines and basic ionic liquids.^[24-27] Other porous materials such as basic metal oxides (such as MgO, Mg-Al mixed oxide), metal phosphates, porous polymers, and g-C₃N₄ have shown interesting results in CO₂ insertion reaction.^[28-32] Moreover, it may be noted that most of the MOFs and zeolite-based catalysts require a high volume of solvents (such as DMF, NMP, CH₂Cl₂, etc.), which makes this process unsustainable. Thus; it is important to develop a suitable catalyst which can be operated in neat condition to produce cyclic carbonate in high selectivity.

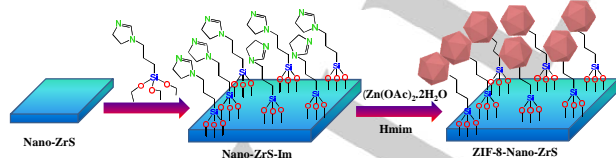
Zeolites are stable and recyclable under liquid phase and gas phase conditions (even under harsh conditions). MOF based catalysts are relatively unstable under liquid phase conditions. Therefore, efforts are being made to develop hybrid and stable porous MOF-zeolite or MOF-silica catalysts for various catalytic applications.^[33-36] Zeolite and MOF based hybrid porous materials would be suitable for the CO₂ insertion reaction. Zeolites have the capability to adsorb CO₂ whereas certain MOFs have the capability to adsorb and activate CO₂. Therefore, the integration of both these porous materials can provide a sustainable solution to the CO₂ insertion reaction. Literature reports suggest that ZIF-8 prepared with Zn ions and 2-methyl imidazole is suitable for the CO₂ activation reaction.^[19, 20] ZIF-8 with sodalite topology has large cages with a diameter of 11.6 Å and a narrow 6-ring pore opening of 3.4 Å.^[37] Such a pore opening is suitable for the CO₂ adsorption.^[38] However, for this reaction, another reactive partner should also be adsorbed

effectively. Thus large surface area zeolite is required. It has been recently shown that nanocrystalline zirconosilicate has the capability to activate epoxide and convert it to amino alcohols via ring-opening reaction.^[39] Literature also suggests that polyethylene amine supported mesoporous zirconosilicate exhibits very good CO₂ adsorption characteristics.^[40, 41] The introduction of optimum amounts of Zr and amine provides suitable acid-base characteristics for efficient CO₂ adsorption and activation.

The objective of this study is to develop zeolite-MOF integrated porous material for CO₂ insertion reaction, for the synthesis of cyclic carbonate under solvent-free conditions in the absence of any co-catalyst. Considering the effective adsorption of CO₂ in ZIF-8 and amorphous zirconosilicate, and high activity of nanocrystalline zirconosilicate in the ring-opening of epoxide, herein, integrated porous material built with nanocrystalline zirconosilicate (designated as Nano-ZrS) with MFI framework structure and ZIF-8 is developed and explored in the production of cyclic carbonates. Further, the developed hybrid porous material is also successful in the synthesis of quinazoline-2,4(1H, 3H)-dione by the CO₂ insertion reaction of 2-amino benzonitrile.

Results and Discussion

In this study ZIF-8-Nano-ZrS, a zeolite-MOF hybrid porous material is prepared by following the synthesis strategy depicted in Scheme 1. First, Nano-ZrS is prepared by following the molar composition 0.93 TEOS/ 0.07 TPHAC/0.02 ZrIPO/ 0.35 TPAOH/40 H₂O under hydrothermal condition using (C₂H₅O)₃SiC₃H₆N(CH₃)₂C₁₆H₃₃]Cl as an additive. Subsequently, Nano-ZrS is functionalized with 3-(2-imidazolyl-1-yl) propyltriethoxysilane to prepare imidazole-functionalized Nano-ZrS, represented as Nano-ZrS-Im. The as-prepared Nano-ZrS-Im is treated with Zn(OAc)₂ and 2-methyl imidazole in water under the ambient condition to prepare ZIF-8-Nano-ZrS. The synthesis details are provided in the experimental section and supporting information section. The characterization details describing the successful formation of the hybrid porous ZIF-8-Nano-ZrS is provided below.



Scheme 1. Schematic presentation for the synthesis of the ZIF-8-Nano-ZrS composite catalyst.

Powdered XRD patterns of parents and their composite material are shown in Figure 1a. The XRD patterns of Nano-ZrS and ZIF-8 are analogous with those reported in the literature for zirconosilicate and ZIF-8 frameworks, respectively.^[39, 21] The XRD pattern of ZIF-8-Nano-ZrS exhibits the characteristic peaks of Nano-ZrS and ZIF-8, which reflects that ZIF-8 framework, is successfully grown on the Nano-ZrS surface without disturbing the structural integrity of the zeolite framework.

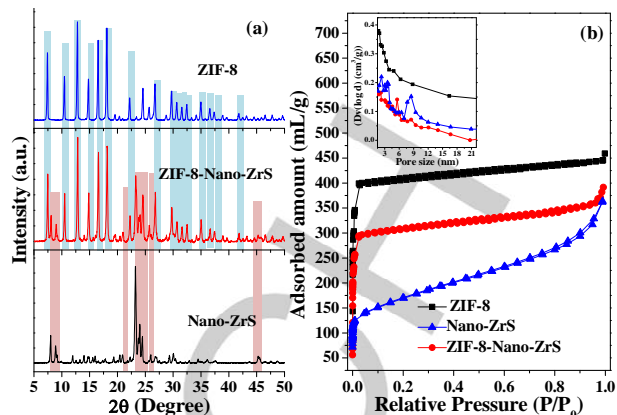


Figure 1. (a) Powder X-ray diffraction patterns and (b) N₂-sorption isotherms of parents and integrated material prepared in this study (Inset shows BJH pore size distribution).

The textural properties of the parents and their integrated material were determined by the nitrogen sorption measurements Figure 1b. Nano-ZrS exhibits type IV isotherm. Significant adsorption below 0.05 (P/P₀) corresponds to the N₂ adsorption in the ZSM-5 micropores. With an increase in the pressure above P/P₀>0.15, a steady increase in the adsorption volume is observed which corresponds to the condensation of N₂ in inter-crystalline mesoporous void space. ZIF-8 exhibits a type I isotherm corresponding to microporous material (Figure 1b). N₂ adsorption in low-pressure range (<0.05 P/P₀) corresponds to the adsorption in the micropores present in ZIF-8. Almost a flat adsorption feature is observed above 0.1 (P/P₀) which suggests that this material has a very low external surface on which further N₂ adsorption would take place on increasing the P/P₀. ZIF-8-Nano-ZrS shows the adsorption feature very similar to that of ZIF-8 but with lower adsorption volume. For this sample, adsorption above 0.9 (P/P₀) suggests the presence of inter-crystalline porosity similar to that of Nano-ZrS.

Table 1. Physico-chemical properties of the different materials investigated in this study.

Sample	Total surface area S _{BET} (m ² /g)	External surface area (m ² /g)	Total pore volume (cm ³ /g)
Nano-ZrS	565	305	0.54
ZIF-8	1290	93	0.59
ZIF-8-Nano-ZrS	884	102	0.52

The pore size distribution suggests that ZIF-8 contains only micropores. Nano-ZrS exhibits the mesopore size distribution in the range of 1.4-4.5 nm and 7-12 nm with a peak maximum at 3.6 nm and 8.6 nm. ZIF-8-Nano-ZrS exhibits pore size distribution somewhat similar to that of ZIF-8. It also shows a pore size distribution in the range of 5 to 6.5 nm with a peak maximum of 5.6 nm, suggesting the presence of intercrystalline pores due to the incorporation of Nano-ZrS in the integrated porous material. Micropore size analysis confirms that hybrid porous material contains the micropores corresponding to MFI and ZIF-8 frameworks. The textural properties of all three materials synthesized in this study are summarized in Table 1.

The highest surface area is obtained for ZIF-8 whereas the lowest surface area is obtained for Nano-ZrS. However, the external surface area is the highest for Nano-ZrS whereas it is the lowest for ZIF-8. The composite material exhibits the surface area and external surface area in between ZIF-8 and Nano-ZrS.

The surface morphology and microstructure of the materials were analyzed using SEM (Figure 2). SEM image of the ZIF-8 exhibits polyhedral like crystal morphology. A spheroid morphology with irregular crystal sizes is observed for the Nano-ZrS. The morphology of ZIF-8-Nano-ZrS is found to be very similar to ZIF-8, which confirms that the imidazole groups on the surface of Nano-ZrS successfully participate in the crystallization process of ZIF-8 framework. The energy dispersive X-ray (EDS) analysis was carried out to investigate the chemical composition of the parent and composite materials (Figure S1). Zn, O, N, and C elements are observed in the EDS spectrum of ZIF-8 whereas Zr, Si, and O elements are observed in the EDS spectrum of Nano-ZrS. However, the two additional peaks corresponding to Si and Zr confirm the growth of the ZIF-8 framework on the surface of zeolite in the ZIF-8-Nano-ZrS (Figure S1).

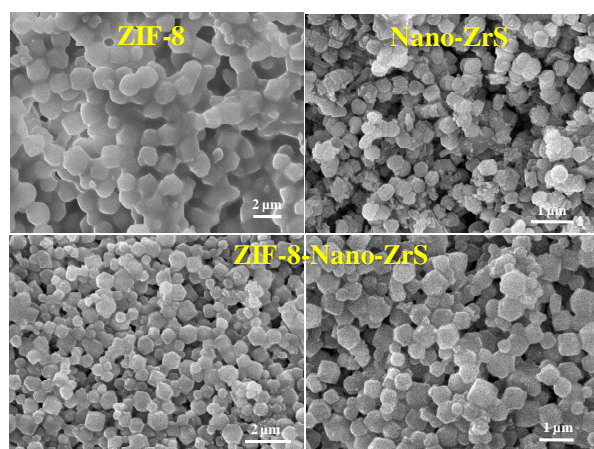


Figure 2. SEM images of parents and their integrated material.

Transmission electron microscopy (TEM) was recorded to distinguish both the frameworks in the ZIF-8-Nano-ZrS (Figure 3). Large rhombic crystal structure (with particle sizes ~430 nm) is observed for the ZIF-8. Very small zeolite nanocrystals are observed for the Nano-ZrS, which shows the lattice fringes with 1.01 nm lattice spacing.

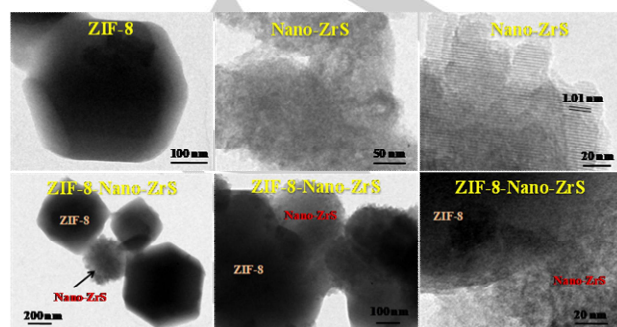


Figure 3. TEM images of parents and their integrated hybrid porous material.

ZIF-8-Nano-ZrS exhibits two distinguished morphologies of different sizes, which correspond to zeolite Nano-ZrS, and MOF ZIF-8. Close inspection shows that the large crystals of ZIF-8 are cross-linked with the Nano-ZrS, which confirms that the ZIF-8 framework is successfully grown on the surface of Nano-ZrS.

The integration of ZIF-8 on the surface of Nano-ZrS was also confirmed by the Fourier transform infrared (FTIR) spectroscopy (Figure 4a). The characteristic peak of Nano-ZrS at 553 cm^{-1} corresponds to the pentasil MFI framework of zirconosilicate zeolite. The absorption peak at 1071 cm^{-1} and 1223 cm^{-1} corresponds to the internal and external asymmetric stretching vibrations of Si-O-Si, respectively while the symmetric stretching of Si-O-Si is observed at 797 cm^{-1} . The characteristic peak of imidazole at 1655 cm^{-1} (C=C stretching) in the Nano-ZrS-Im confirms the functionalization of imidazole on the surface of Nano-ZrS. ZIF-8 shows the adsorption at 423 cm^{-1} which indicates that Zn^{2+} chemically interacts with the N atom of the HMIM linker and forms the imidazolate framework. Furthermore, the absorption bands in the region of 1285-1490 cm^{-1} correspond to ring stretching. The C-N and C-H bending vibrations are observed at 992 and 760 cm^{-1} , respectively whereas C-N stretching vibration is observed at 1143 cm^{-1} . All the characteristic peaks of zeolite Nano-ZrS and MOF ZIF-8 are observed in the FTIR spectrum of ZIF-8-Nano-ZrS, which indicates that the ZIF-8 framework is successfully grown on the surface of Nano-ZrS (Figure 4a).

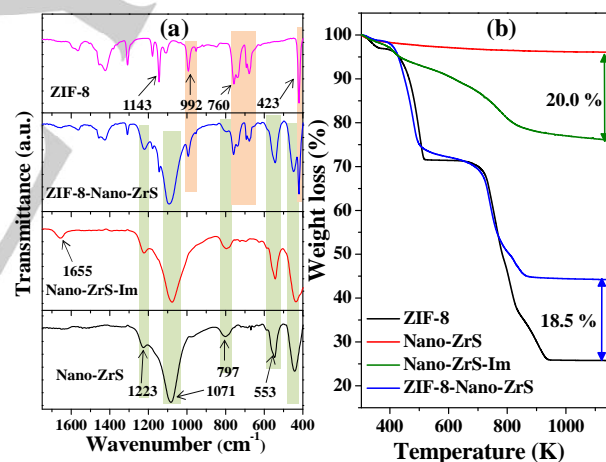


Figure 4. (a) FT-IR spectra, and (b) thermograms of parents and their integrated material prepared in this study.

Thermogravimetric analysis (TGA) was performed to investigate the amount of individual frameworks in the ZIF-8-Nano-ZrS hybrid material (Figure 4b). No significant weight loss is observed in the Nano-ZrS, which indicates the high stability of the zeolite framework. The weight loss in Nano-ZrS-Im corresponds to the removal of functionalized linker on the surface of zirconosilicate. The difference between the weight loss of Nano-ZrS-Im and Nano-ZrS is related to the amount of imidazole linker anchored to the surface of Nano-ZrS (Figure 4b). However, two weight losses are observed in the ZIF-8. The first weight loss corresponds to the removal of physisorbed H_2O molecules (up to 500 K). The second weight loss is related to the degradation of the framework to form ZnO. The difference in

the weight loss between ZIF-8 and ZIF-8-Nano-ZrS (18.5 wt%) corresponds to the amount of zirconosilicate present in the composite material (Figure 4b)

Catalytic Activity

For the CO₂ insertion reaction, the CO₂ should be adsorbed and effectively activated on the catalyst surface. Thus it is important to investigate the CO₂ adsorption in all the samples. CO₂ adsorption isotherm of parents and their integrated material is shown in Figure 5. CO₂ adsorption experiment was performed at 298 K after evacuating the materials at 423 K before the CO₂ adsorption. With an increase in the CO₂ pressure in the range of 0 to 1 bar, the CO₂ adsorption increased for all the materials. Nano-ZrS shows the highest adsorption of CO₂ in the entire pressure range (0.0-1.0 bar) which is consistent with the literature reports with amorphous zirconosilicate.^[40] ZIF-8 exhibits the lowest CO₂ adsorption among various materials investigated in this study. The CO₂ adsorption with ZIF-8-Nano-ZrS falls in between Nano-ZrS and ZIF-8. Higher adsorption of CO₂ in Nano-ZrS is due to the presence of Zr in MFI lattice which is known to enhance the CO₂ adsorption.^[40] Moreover, intercrystalline mesopores, micropores with a wider pore window (0.54 nm), and a larger external surface area of Nano-ZrS than ZIF-8 are responsible for the higher CO₂ adsorption in the material. The integrated material ZIF-8-Nano-ZrS contains 18.5 % Nano-ZrS, therefore, it exhibits more CO₂ adsorption than ZIF-8. The CO₂ adsorption capacities of Nano-ZrS, ZIF-8, and ZIF-8-Nano-ZrS at 1 bar are determined to be 50.4 cm³g⁻¹, 25.7 cm³g⁻¹, and 36.5 cm³g⁻¹, respectively.

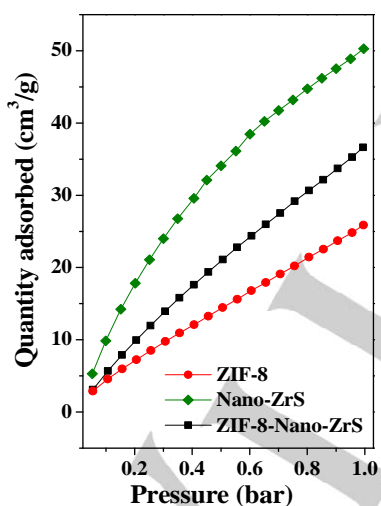


Figure 5. CO₂ adsorption isotherms of parents and integrated porous material prepared in this study at 298 K.

The activation of CO₂ is related to the chemisorption of CO₂. Thus, temperature-programmed desorption of CO₂ (CO₂-TPD) measurements for all catalysts were conducted. The CO₂-TPD profiles of the parents and their composite material are presented in Figure S2. The CO₂ desorptions for ZIF-8 take place in the range of 325-425 K and 425-563 K, which correspond to weak and medium basic sites, respectively. Nano-

ZrS shows weak CO₂-desorption above 400 K. However, ZIF-8-Nano-ZrS shows weak CO₂ desorption in 325-425 K, but very high CO₂ desorption is observed in the range of 425-563, suggesting that the material has stronger basicity than ZIF-8. Total basicity of ZIF-8-Nano-ZrS (1.3 μmol/g) is more than that of their parents materials, ZIF-8 (1.1 μmol/g) and Nano-ZrS (0.7 μmol/g). Thus the higher amount of CO₂ adsorption/desorption and stronger basic sites present in ZIF-8-Nano-ZrS are expected to provide better activity in the CO₂ insertion reactions.

For CO₂ insertion reaction in the synthesis of cyclic carbonate, only high CO₂ adsorption/desorption is not sufficient condition. It is the effective CO₂ adsorption on the catalyst surface (determined from CO₂-TPD), and the ring-opening of epoxide by the adsorption of epoxide on the Lewis acid sites of the catalyst, both are required. Pyridine adsorbed FT-IR measurement was carried out to confirm the presence of Lewis acid sites in the material (Figure S3). Nano-ZrS exhibits a strong peak at 1444 cm⁻¹ which corresponds to pyridine bonded to the Lewis acid sites of the material. The peak at 1596 cm⁻¹ is due to H-bonded pyridine with surface Si-OH groups present in this material. In the case of ZIF-8, only weak adsorption at 1439 cm⁻¹ is observed, which suggests that this material has very weak Lewis acidity. Moreover, no H-bonded pyridine peak is observed for this material, confirming the absence of any surface -OH group in this material (Figure S3). In the case of ZIF-8-Nano-ZrS, weak absorptions at 1439 cm⁻¹ and 1591 cm⁻¹ confirm the presence of Lewis acid sites and H-bonded pyridine, respectively, which further confirms the integration of these two porous materials (Figure S3).

The catalytic activity data presented here provide exact information about the activity of the catalysts under optimized reaction conditions. Nano-ZrS is found to be almost inactive for this reaction (Table 2, Entry 2). Based on CO₂ adsorption data at 298 K (discussed above) and effective ring opening of epoxide (cited previously),^[39] this catalyst should have provided the best activity. The inferior activity of Nano-ZrS in cyclic carbonate synthesis clearly suggests that CO₂ is not effectively adsorbed (as confirmed from CO₂-TPD) on Nano-ZrS under the experimental condition, and not suitable for the CO₂ insertion reaction. The activity of Nano-ZrS-Im is somewhat better when compared to Nano-ZrS, which suggests that CO₂ is partially adsorbed and present on the catalyst surface due to the weak interaction between imidazole and CO₂ molecules (Table 2, Entry 3). Since only a low concentration of imidazole is present on the Nano-ZrS-Im, therefore, the activity is very poor. The activity of ZIF-8 is very good under the optimized reaction condition (Table 2, Entry 4). Moreover, excellent activity is achieved using ZIF-8-Nano-ZrS (Table 2, Entry 5). This is due to the effective adsorption of CO₂ in the material and also due to the effective activation of CO₂ by the imidazole linker present in the material. In our previous report, we have demonstrated that Zn based MOFs including ZIF-8 was not good for the ring-opening of the epoxide during the amination reaction of the epoxide.^[42]

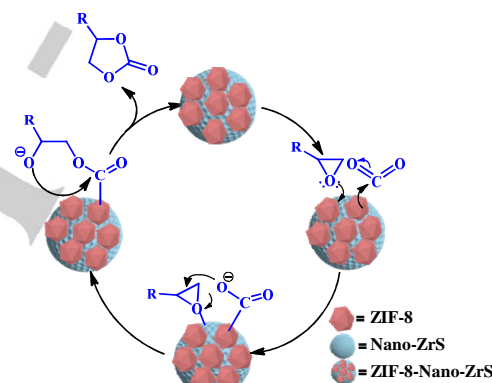
Table 2. Cycloaddition of CO₂ to epoxide using different catalysts prepared in this study.

E. N. o.	Catalyst	Reactant	Time (h)	Conv. (%)	Product Sel. (%)	TON ^a
1.	-	ECH	2	0	0	-
2.	Nano-ZrS	ECH	2	<1	-	-
3.	Nano-ZrS-Im	ECH	2	9.3	80.5	9.8
4.	ZIF-8	ECH	2	70.2 (65.8) ^c	97.3	60.6
5.	ZIF-8-Nano-ZrS	ECH	2	96.8 (89.5) ^c	94.9	102.5
6.	ZIF-8-Nano-ZrS	PO	2	58.2	97.4	61.6
7.	ZIF-8-Nano-ZrS	PO	8	87.9	93.7	93.0
8.	ZIF-8-Nano-ZrS	SO	2	35.4	95.6	37.5
9.	ZIF-8-Nano-ZrS	SO	8	76.6 (70.5) ^c	94.8	81.1
10.	ZIF-8-Nano-ZrS ^b	ECH	2	92.5	94.7	97.9

Reaction condition: Epoxide (38 mmol), catalyst (100 mg), reaction temperature (393 K), reaction time (2 h), CO₂ pressure (10 bar). ^aTON= Turn over number (moles of product/moles of catalyst), ^bCatalytic data obtained after the fifth recycles, and ^cisolated yield. ECH= Epichlorohydrin, PO = Propylene oxide, and SO = Styrene oxide.

At the same time, Zr based MOF and nanocrystalline zirconosilicates have been reported to exhibit very good activity in the ring-opening reaction of the epoxide.^[39] If the activity of nanocrystalline zirconosilicates and Uio-66 is considered, the activity of nanocrystalline zirconosilicate is more in the ring-opening reaction of the epoxide.^[39,41] Thus, due to the weak activation of epoxide by ZIF-8, the activity of ZIF-8 in the CO₂ insertion reaction to produce chloropropene carbonate is found to be moderate (Table 2, entry 4). Due to the presence of integrated framework, simultaneous activation of epoxide by Nano-ZrS and effective adsorption and activation of CO₂ by ZIF-8, the activity of ZIF-8-Nano-ZrS is found to be excellent (Table 2, entry 5). GC-MS data show that the side product formed during the CO₂ insertion reaction with epichlorohydrin is 1-chloropropanol/2-chloropropanol. It may be noted that the reaction is performed in the neat condition and in the absence of any co-catalyst. The influence of various reaction parameters, such as reaction time, temperature and catalyst amount is investigated (Figure S4). With an increase in reaction temperature, the epoxide conversion increases but the selectivity of cyclic carbonates marginally decrease. However, the reaction proceeds well at 393 K. Above 393 K, only a marginal increase in the epoxide conversion is obtained with a further decrease in the carbonate selectivity. Thus 393 K is chosen for further optimization. The influence of the reaction time suggests that better selectivity and carbonate yield are obtained after 2 h of the reaction with epichlorohydrin (Figure S4). With an increase in the catalyst amount from 50 mg to 150

mg, the activity of catalyst increases. Above 100 mg catalyst, no significant increase in epoxide conversion is obtained. Finally, the influence of CO₂ pressure is also investigated in the range of 2.5 bar to 12.5 bar. With an increase in the CO₂ pressure, the epichlorohydrin conversion increases up to 10 bar. With a further increase in the CO₂ pressure, no significant increase in the epichlorohydrin conversion is obtained. Thus, 393 K, 100 mg catalyst, 10 bar CO₂ pressure, and 2 h reaction time are optimized for CO₂ insertion reaction of epichlorohydrin. The activation energy E_a for this reaction is calculated for ZIF-8 and ZIF-8-Nano-ZrS using the Arrhenius plot (ln k versus $1/T$, Figure S5) by following the first-order kinetics because the catalyst amount is constant and the high CO₂ concentration is taken when compared to the epichlorohydrin (which can also be considered constant). The activation energies for ZIF-8 and ZIF-8-Nano-ZrS are calculated to be 50.8 kJ/mol and 48.8 kJ/mol, respectively. Lower activation energy further confirms the higher activity of ZIF-8-Nano-ZrS when compared to ZIF-8 in the CO₂ insertion reaction of epichlorohydrin.

**Scheme 2.** A plausible reaction mechanism for the insertion reaction of CO₂ into epoxide.

Having optimized the reaction condition, the applicability of the composite catalyst is further investigated with different aliphatic and aromatic epoxides. Lower cyclic carbonate yield is obtained using propylene oxide and styrene oxide (Table 2, Entries 6, 8). Thus, the reaction duration for these substrates is increased to obtain a good product yield (Table 2, Entries 7, 9). To investigate the stability of the composite catalyst, ZIF-8-Nano-ZrS is recycled five times. No significant change in the activity is observed even after five recycles (Table 2, Entry 1 and Figure S6). XRD (Figure S7), FT-IR (Figure S7), and SEM (Figure S7) investigations confirm that the recycled catalyst is stable after the five recycles.

In this study, ZIF-8 framework is integrated with nanocrystalline zirconosilicate by functionalization of nanocrystalline zirconosilicate with imidazole, that participates in the growth of ZIF-8 through the imidazole surface-functionalized nanocrystalline zirconosilicates. Scheme 2 shows the plausible mechanism for the CO₂ insertion reaction of the epoxide. The presence of bi-functional sites in the ZIF-8-Nano-ZrS attributes the efficiency of the catalyst. The Lewis acid sites in ZIF-8-Nano-

ZrS (Zn/Zr center, Zr is more effective than Zn) adsorb and activate the epoxide. Whereas; the basic sites (imidazole linker) effectively activate the adsorbed CO₂ (CO₂ is more adsorbed in Nano-ZrS but effectively adsorbed in ZIF-8). Thus, the simultaneous adsorption and activation of epoxide and CO₂ in close proximity on ZIF-8-Nano-ZrS facilitate the CO₂ insertion into epoxide to produce cyclic carbonate. The activity of the present catalyst is compared with other similar catalysts reported in the literature. The comparative data suggests that the developed catalyst in this study exhibits better or comparable activity even in the absence of any co-catalyst (Table S1).

After achieving the excellent activity in the cyclic carbonate synthesis, the applicability of the ZIF-8-Nano-ZrS is further investigated in the synthesis of quinazoline-2,4(1H, 3H)-dione. Quinazoline-2,4(1H, 3H)-dione is produced by the addition of CO₂ to 2-aminobenzonitrile. The influence of solvent demonstrated in our previous studies suggests that DMF is the best solvent for this reaction not only with respect to the 2-aminobenzonitrile conversion but also with respect to the isolation of the product.^[26] Thus in this study, the reaction parameters are evaluated in DMF solvent using 2-amino benzonitrile as a model substrate. The influence of reaction parameters such as type of catalyst, reaction temperature, catalyst amount, and reaction pressure is shown in Figure 6. In this reaction, only quinazoline-2,4(1H, 3H)-dione is obtained as the selective product which is confirmed by the ¹H-NMR (Figure S8). Nano-ZrS is found to be inactive for this reaction (Figure 6a). However, low product yield is obtained using ZIF-8 catalyst (Figure 6a). The highest product yield is obtained using ZIF-8-Nano-ZrS (Figure 6a). With an increase in the reaction temperature, pressure, and catalyst amount, the product yield increases (Figure 6b-d). The excellent yield of 83 % is obtained when the reaction is conducted at 433 K and 40 bar pressure using 150 mg of catalyst for 12 h. Comparative catalytic activity shown in Figure 6a suggests that the synthesis of quinazoline-2,4(1H, 3H)-dione facilitates by the basic sites of the catalyst. The low activity of ZIF-8 suggests that the basic sites in the ZIF-8 frameworks are not easily accessible to the reactant molecules. ZIF-8 grown on Nano-ZrS provides more isolated and dispersed sites. Moreover, the adsorption of 2-aminobenzonitrile is facilitated on the Nano-ZrS sites through weak coordination between the amino groups of 2-aminobenzonitrile and Lewis acidic Zr sites.

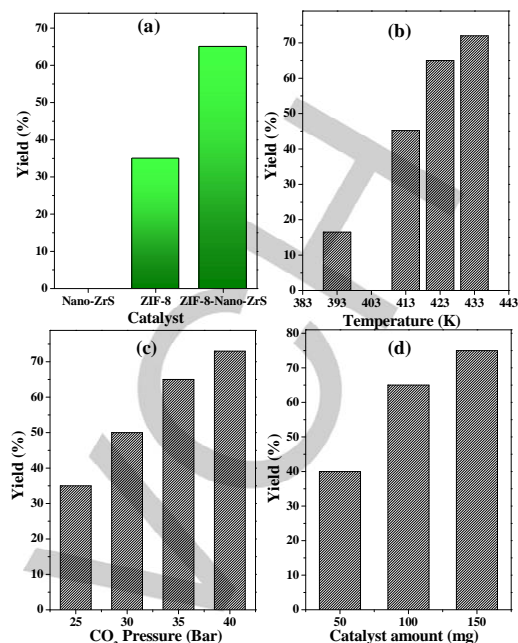


Figure 6. Influence of reaction parameters, (a) catalyst, (b) temperature, (c) CO₂ pressure, and (d) catalyst amount in the synthesis of quinazoline-2,4(1H, 3H)-dione by the insertion reaction of CO₂ to 2-aminobenzonitrile. Reaction condition: (a) 2-aminobenzonitrile (2 mmol), DMF (10 mL), temperature (423 K), CO₂ pressure (35 bar), catalyst (100 mg), and time (12 h); (b) 2-aminobenzonitrile (2 mmol), DMF (10 mL), CO₂ pressure (35 bar), catalyst (100 mg), and time (12 h); (c) 2-aminobenzonitrile (2 mmol), DMF (10 mL), temperature (423 K), catalyst (100 mg), and time (12 h); (d) 2-aminobenzonitrile (2 mmol), DMF (10 mL), temperature (423 K), CO₂ pressure (35 bar), and time (12 h).

Thus, the efficient adsorption and dispersed basic sites present in the ZIF-8-Nano-ZrS are responsible for the excellent activity of ZIF-8-Nano-ZrS in quinazoline-2,4(1H, 3H)-dione synthesis. Scheme S1 shows the plausible reaction mechanism for the synthesis of quinazoline-2,4(1H, 3H)-dione using ZIF-8-Nano-ZrS as the catalyst. The acidic proton of the amino group in 2-aminobenzonitrile is abstracted by the basic site of the catalyst and generates the intermediate 1a. Furthermore, similar to cyclic carbonate synthesis, the basic sites in the catalyst adsorb and activate the CO₂ molecules. Then, the intermediate 1a undergoes a nucleophilic attack to active CO₂ molecule and form intermediate 1b, which attacks—CN group and generates intermediate 1c. Ring-opening (intermediate 1d) followed by intramolecular cyclization leads to the formation of intermediate 1e, which undergoes the tautomerization and generates stable cyclic amide quinazoline-2,4(1H, 3H)-dione.

Conclusion

2-Methyl imidazole based ZIF-8 was integrated with nanocrystalline zirconosilicate to prepare integrated porous structure. XRD and FT-IR confirm the formation of integrated material. Parent ZIF-8 exhibited the large micropore surface area, whereas; the Nano-ZrS exhibited a large external surface

area. Transmission electron microscopic investigation revealed that the integrated porous material was built with large ZIF crystals (400-600 nm) and very small size Nano-ZrS nanocrystals (10-20 nm). ZIF-8 exhibited moderate activity in the CO₂ insertion reaction in epichlorohydrin to form cyclic carbonate due to the weak Lewis acidity which facilitates the ring-opening of the epoxide. The effective CO₂ adsorption in ZIF-8 was due to the 2-methyl imidazole building moiety and large micropore area. An integrated porous material, ZIF-8-Nano-ZrS, exhibited excellent activity in the cyclic carbonate synthesis because Nano-ZrS exhibited excellent ring-opening capability due to the presence of Lewis acid sites and effective adsorption of CO₂ by ZIF-8 sites present in the material. Simultaneous, effective adsorption of CO₂ and epoxide in the close proximity on integrated porous material was responsible for the excellent activity of this material in neat condition. The excellent yield of the product under mild reaction conditions in the absence of any co-catalyst and efficient recyclability are other attractive features of this catalytic process. Moreover, the integrated porous material exhibited very good activity in the synthesis of quinazoline-2,4(1H, 3H)-dione, which was much higher than their parent porous materials, ZIF-8 and Nano-ZrS. We are sure that such an approach to developing MOF-zeolite integrated material will attract the significant attention of the materials chemist and catalysis researchers to develop similar types of materials for the appointed applications.

Experimental Section

Synthesis of ZIF-8-Nano-ZrS nanocomposite

For the synthesis of ZIF-8 integrated nanocrystalline zirconosilicate (ZIF-8-Nano-ZrS), initially nanocrystalline zirconosilicate (Nano-ZrS) was synthesized by following the reported procedure.^[39] In a typical synthesis of nanocrystalline zirconosilicate, zirconium (IV) isopropoxide (ZrIPO, 0.18 g) was added dropwise to tetraethylorthosilicate (TEOS, 3.94 g) and the resultant solution was stirred for 15 min under ambient condition until a clear solution was formed (solution A). In a separate bottle, [(C₂H₅O)₃SiC₃H₆N(CH₃)₂C₁₆H₃₃]Cl (TPHAC, 0.72 g) and tetrapropylammonium hydroxide (TPAOH, 3.54 g) was added into the deionized water (4.3 g) (Solution B). Then, solution A was added to solution B, followed by the addition of 8 mL deionized water. The resultant mixture was slowly stirred at ambient conditions for 6 h. The resultant molar composition was 0.93 TEOS/ 0.07 TPHAC/0.02 ZrIPO/ 0.35 TPAOH/40 H₂O. Next, the resultant reaction mixture was transferred to a Teflon-lined stainless steel autoclave and hydrothermally treated at 443 K under the stirring condition for 5 days. After the crystallization, the obtained solid product was filtered, washed with distilled water, and dried at 373 K. To remove the incorporated surfactant molecules, the solid material was calcined at 823 K for 6 h. The final obtained material was designated as Nano-ZrS.

Then, the external surface of Nano-ZrS was functionalized with an imidazole linker. 0.136 g of 3-(2-imidazolyl-1-yl) propyltriethoxysilane and 0.5 g Nano-ZrS were added to 12.5 mL dry toluene and the reaction mixture was refluxed for 24 h. The resultant mixture was filtered, washed with dichloromethane and dried in a vacuum oven at 373 K for 12 h

to obtain imidazole functionalized Nano-ZrS (designated as (Nano-ZrS-Im).

For the preparation of ZIF-8-Nano-ZrS composite, the first 0.2 g of Nano-ZrS-Im was added to a solution containing 0.219 g of Zn(OAc)₂ and 10 mL of deionized water. The resultant mixture was stirred under the ambient condition for 1 h (solution A). In a separate container, 2.46 g of 2-methyl imidazole (Hmim) was dissolved in deionized water (30 mL) and stirred at room temperature for 1 h (solution B). Then, solution B was added to solution A and the resultant mixture was slowly stirred under the ambient condition for 24 h. After the reaction, the cloudy aqueous suspension was centrifuged, washed several times with methanol and dried in a vacuum oven at 373 K for 12 h to obtain ZIF-8-Nano-ZrS.

For a comparative study, ZIF-8 was also prepared by following the same procedure without adding Nano-ZrS-Im.

The details of the instruments and methods used for materials characterization are provided in the Electronic Supporting Information Section.

Catalytic activity

The details for the procedure of the catalytic reactions are provided in the Electronic Supporting Information Section.

Acknowledgments

The work presented in this manuscript is supported by DST-SERB, New Delhi (EMR/2016/001408). PR acknowledges the Director's Fellowship provided by the IIT Ropar. RS thank IIT Ropar for providing grants through the Faculty Research Innovation Award.

Conflicts of interest

The authors declare no competing financial interest.

Keywords: CO₂ activation • Metal-organic framework • Nanocrystalline Zeolite • Integrated Porous Framework • Insertion Reactions

- [1] G. T. Narisma, A. J. Pitman, *Earth Interact.* **2006**, *10*, 1-27.
- [2] E. S. Sanz-Perez, C. R. Murdock, S. A. Didas, C.W. Jones, *Chem. Rev.* **2016**, *116*, 11840-11876.
- [3] S. A. Didas, S. Choi, W. Chaikittisilp, C.W. Jones, *Acc. Chem. Res.* **2015**, *48*, 2680-2687.
- [4] B. Dutcher, M. Fan, A. G. Russell, *ACS Appl. Mater. Interfaces* **2015**, *7*, 2137-2148.
- [5] Q. Wang, J. Luo, Z. Zhong, A. Borgna, *Energy Environ. Sci.* **2011**, *4*, 42-55.
- [6] R. Banerjee, H. Furukawa, D. Britt, C. Knobler, M. O'Keeffe, O.M. Yaghi, *J. Am. Chem. Soc.* **2009**, *131*, 3875-3877.
- [7] J. Liu, P. K. Thallapally, B. P. McGrail, D. R. Brown, J. Liu, *Chem. Soc. Rev.* **2012**, *41*, 2308-2322.
- [8] V. Presser, J. McDonough, S. H. Yeon, Y. Gogotsi, *Energy Environ. Sci.* **2011**, *4*, 3059-3066.
- [9] J. Ma, N. Sun, X. Zhang, N. Zhao, F. Xiao, W. Wei, Y. Sun, *Catal. Today*, **2009**, *148*, 221-231.
- [10] M. Aresta, *Carbon Dioxide as Chemical Feedstock*, 1 edition, Wiley-

- VCH, **2010**.
- [11] J. S. Chang, V. P. Vislovskiy, M. S. Park, D. Y. Hong, J. S. Yoo, S. E. Park, *Green Chem.* **2003**, *5*, 587-590.
- [12] J. E. Hallgren, *Patent US4410464A*, **1982**.
- [13] A. J. Kamphuis, F. Picchioni, P. P. Pescarmona, *Green Chem.* **2019**, *21*, 406-448.
- [14] W. G. Tu, Y. Zhou, Z. G. Zou, *Adv. Mater.* **2014**, *26*, 4607-4626.
- [15] K. C. Waugh, *Catal. Today.* **1992**, *15*, 51-75.
- [16] D. Bonenfant, M. Kharoune, P. Niquette, M. Mimeault, R. Hausler, *Sci. Technol. Adv. Mater.* **2008**, *9*, 013007-013013.
- [17] F. Akhtar, Q. Liu, N. Hedin, L. Bergstrom, *Energy Environ. Sci.* **2012**, *5*, 7664-7673.
- [18] S. Xiang, Y. He, Z. Zhang, H. Wu, W. Zhou, R. Krishna, B. Chen, *Nat. Commun.* **2012**, *3*, 954-962.
- [19] A. C. Kathalikkattil, R. Babu, J. Tharun, R. Roshan, D. W. Park, *Catal. Surv Asia* **2015**, *19*, 223-235.
- [20] C. M. Miralda, E. E. Macias, M. Zhu, P. Ratnasamy, M. A. Carreon, *ACS Catal.* **2012**, *12*, 180-183.
- [21] P. Rani, R. Srivastava, *New J. Chem.* **2017**, *41*, 8166-8177.
- [22] T. Lescouet, C. Chizallet, D. Farrusseng, *ChemCatChem* **2012**, *4*, 1725-1728.
- [23] P. Patel, B. Parmar, R. I. Kureshy, N. H. Khan, E. Suresh, *Dalton Trans.* **2018**, *47*, 8041-8051.
- [24] R. Srivastava, D. Srinivas, P. Ratnasamy, *J. Catal.* **2005**, *233*, 1-15.
- [25] R. Srivastava, D. Srinivas, P. Ratnasamy, *Catal. Lett.* **2003**, *91*, 133-139.
- [26] B. Sarmah, R. Srivastava, *Ind. Eng. Chem. Res.* **2017**, *56*, 8202-8215.
- [27] B. Sarmah, B. Satpati, R. Srivastava, *J. Colloid Interface Sci.* **2017**, *493*, 307-316.
- [28] A. H. Chowdhury, P. Bhanja, N. Salam, A. Bhaumik, S. M. Islam, *Mol. Catal.* **2018**, *460*, 46-54.
- [29] A. H. Chowdhury, I. H. Chowdhury, S. M. Islam, *Ind. Eng. Chem. Res.* **2019**, *58*, 11779-11786.
- [30] S. Bhunia, R. A. Molla, V. Kumari, S. M. Islam, A. Bhaumik, *Chem. Commun.* **2015**, *51*, 15732-15735.
- [31] S. Samanta, R. Srivastava, *Sustain. Energy Fuels* **2011**, *1*, 1390-1404.
- [32] K. Yamaguchi, K. Ebitani, T. Yoshida, H. Yoshida and K. Kaneda, *J. Am. Chem. Soc.*, **1999**, *121*, 4526-4527.
- [33] P. Rani, R. Srivastava, *J. Colloid Interface Sci.* **2019**, *557*, 144-155.
- [34] P. Rani, R. Srivastava, *Sustain. Energy Fuels* **2018**, *2*, 1287-1298.
- [35] D. Suttiapat, W. Wannapakdee, T. Yuthalekha, S. Ittisanronnachai, T. Ungpittagul, K. Phomphrai, S. Bureekaew, C. Wattanakit, *ACS Appl. Mater. Interfaces* **2018**, *10*, 16358-16366.
- [36] L. Lin, T. Zhang, X. Zhang, H. Liu, K. L. Yeung, J. Qiu, *Ind. Eng. Chem. Res.* **2014**, *53*, 10906-10913.
- [37] D. F. Jimenez, S. A. Moggach, M. T. Wharmby, P. A. Wright, S. Parsons, T. Düren, *J. Am. Chem. Soc.* **2011**, *133*, 8900-8902.
- [38] A. Phan, C. J. Doonan, F. J. Uribe-Romo, C. B. Knobler, M. O'Keeffe, O. M. Yaghi, *Acc. Chem. Res.* **2010**, *43*, 58-67.
- [39] R. Kore, R. Srivastava, B. Satpati, *ACS Catal.* **2013**, *3*, 2891-2904.
- [40] Y. Kuwahara, D. Y. Kang, J. R. Copeland, N. A. Brunelli, S. A. Didas, P. Bollini, C. Sievers, T. Kamegawa, H. Yamashita, C. W. Jones, *J. Am. Chem. Soc.* **2012**, *134*, 10757-10760.
- [41] B. L. Newalkar, J. Olanrewaju, S. Komarneni, *J. Phys. Chem. B* **2001**, *105*, 8356-8360.
- [42] P. Rani, R. Srivastava, *RSC Adv.* **2015**, *5*, 28270-28280.

Table of Contents



Efficient ring opening of epoxide by nanocrystalline zirconosilicate and effective adsorption of CO₂ by ZIF-8 led to prepare the integrated porous material, ZIF-8-Nano-ZrS, which exhibited excellent activity in the CO₂ insertion of epoxide for cyclic carbonate synthesis under a neat condition in the absence of any co-catalyst. The catalyst exhibited excellent activity in the CO₂ insertion reaction to prepare quinazoline-2,4(1H,3H)-dione.